

## Formation and capacitance properties of Ti-Al composite oxide film on aluminum

YAO Lei(姚 雷), LIU Jian-hua(刘建华), YU Mei(于 美), LI Song-mei(李松梅), WU Hao(吴 昊)

School of Materials Science and Engineering, Beihang University, Beijing 100191, China

Received 12 May 2009; accepted 18 June 2009

**Abstract:** Al specimens were covered with TiO<sub>2</sub> film by sol-gel dip-coating and then anodized in ammonium adipate solution. The structure, composition and capacitance properties of the anodic oxide film were investigated by transmission electron microscopy (TEM), Auger electron spectroscopy (AES), X-ray diffractometry (XRD) and electrochemical impedance spectroscopy (EIS). It was found that an anodic oxide film with a dual-layer structure formed between TiO<sub>2</sub> coating and Al substrate. The film consisted of an inner Al<sub>2</sub>O<sub>3</sub> layer and an outer Ti-Al composite oxide layer. The thickness of layers varied with the number of times of sol-gel dip-coating. The capacitance of anodic oxide films formed on coated specimens was at most 80% higher than that without TiO<sub>2</sub>. In film formation mechanism, it was claimed that the formation of composite oxide film was mainly affected by the structure of micro-pores network in TiO<sub>2</sub> coating which had an influence on Al<sup>3+</sup> and O<sup>2-</sup> ions transport during the anodizing.

**Key words:** Al electrolytic capacitor; composite oxide film; anodized dielectric film; sol-gel coating; capacitance property

### 1 Introduction

Aluminum electrolytic capacitors are widely used in electric and electronic devices. Recent development of mobile electronic devices, such as notebook computers and portable telephones, requires very small electrolytic capacitors with high electric capacitance[1]. Barrier type anodic oxide film formed on Al plays an important role as dielectric film in Al electrolytic capacitor, and its capacitance properties have a great effect on the performance of the capacitor.

The electric capacitance,  $C$ , of anodic oxide film on Al is expressed by

$$C = \varepsilon_0 \cdot \varepsilon \cdot S / d \quad (1)$$

where  $\varepsilon_0$  represents the vacuum permittivity;  $\varepsilon$  represents the specific dielectric constant of the anodic oxide films;  $S$  is the effective surface area; and  $d$  is the film thickness.

As increasing  $\varepsilon$  is a new way to improve capacitance, recently there is a growing interest in the formation of composite oxide films by incorporating valve metal oxides or other materials with high dielectric constant into Al anodic oxide film[1–13]. Several researchers prepared Zr-Al[1, 3], Si-Al[4–5], Nb-Al[6], (Ba<sub>0.5</sub>Sr<sub>0.5</sub>)TiO<sub>3</sub>-Al[7] and Bi<sub>4</sub>Ti<sub>3</sub>O<sub>12</sub>-Al[8] composite

oxide films on Al substrate by sol-gel coating and anodizing. However, in these studies, the growth mechanism of the composite oxide film lacked detailed discussion and the effect of the sol-gel coating was not considered.

TiO<sub>2</sub> has a high relative dielectric constant, showing 48 for anatase and 110–117 for rutile structure[14]. It is expected that incorporation of TiO<sub>2</sub> into Al anodic oxide film may form a Ti-Al composite oxide film with high dielectric constant and improve the capacitance.

In the present work, a Ti-Al composite oxide film was attempted by using the method of sol-gel coating and subsequent anodizing. The structure, composition and capacitance properties of the film were investigated. An anodization model was presented; and as for the formation mechanism of the composite oxide film, function and effects of TiO<sub>2</sub> coating were discussed.

### 2 Experimental

#### 2.1 Preparation of Ti-Al composite oxide film

The specimen (2 cm × 2.5 cm with handle) was cut from highly pure Al foil (99.99%) and ultrasonically cleaned in dehydrated ethanol. TiO<sub>2</sub> film was applied to the specimens via a sol-gel dip-coating method. TiO<sub>2</sub> sol

was prepared by mixing tetrabutyl titanate, deionized water, hydrochloric acid and dehydrated ethanol at the molar ratio of 1:5.8:1.1:46.8, and then the sol was stirred for 24 h. Specimens were immersed in the sol for 60 s and drawn out at a speed of 3 mm/s. After being air-dried at the room temperature, the specimens were heated in a furnace at 773 K for 10 min. The cycle of dip-coating and heating was repeated once to four times ( $n=1-4$ ).

Coated specimens were anodized to 100 V with a constant current of 2 mA/cm<sup>2</sup> in 13% (mass fraction) ammonium adipate solution at 358 K. After the selected voltage was reached, the anodization continued for 10 min while the voltage was held constant and the current was allowed to decay. The specimen without TiO<sub>2</sub> was anodized under the same conditions for comparison.

## 2.2 Micro-morphology and structure analysis

TiO<sub>2</sub> film and anodic oxide film were stripped in 10% (mass fraction) Br<sub>2</sub> methanol solution from coated specimens before and after anodizing, respectively. Then, the films were observed by TEM (Jeol JEM-2100F). The depth profile of component elements in the Ti-Al composite oxide film was examined by AES (Perkin-Elmer PHI-700). The composition of TiO<sub>2</sub> film was identified by XRD (Rigaku D/max-2200).

## 2.3 Capacitance measurement

The specific capacitance of the anodic oxide film was measured in 13% (mass fraction) ammonium adipate solution at 293 K using a general LCR meter. Dielectric properties of the anodic oxide film were examined by EIS measurement. In EIS measurement, specimens were immersed in 13% ammonium adipate solution at 293 K, and 10 mV of sinusoidal voltage in 10<sup>-3</sup>–10<sup>5</sup> Hz range was applied. The EIS results were analysed using the software ZSimpWin<sup>®</sup> 3.20 (EChem Software).

## 3 Results and discussion

### 3.1 Composition of TiO<sub>2</sub> film

TiO<sub>2</sub> powder was obtained by heating the aforementioned sol at 773 K for 2 h and its XRD pattern is shown in Fig.1. It was indicated that the powder mainly consisted of anatase and only a little amount of rutile appeared. Fig.2 shows XRD patterns of specimen without (Fig.2(a)) and with (Fig.2(b)) TiO<sub>2</sub> coating. The derived film on Al substrate consisted of anatase, which was in accordance with Fig.1. The dielectric constant of anatase type TiO<sub>2</sub> was lower than that of the rutile type. However, the annealing temperature of sol-gel derived TiO<sub>2</sub> film was over 973 K[15] for anatase to transform mostly into rutile. It was unable to obtain rutile type film on Al substrate in this study since the melting point of Al is 933 K.

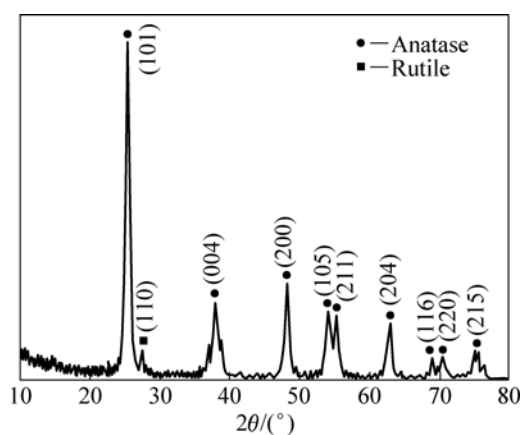


Fig.1 XRD pattern of TiO<sub>2</sub> powder obtained by heating sol at 773 K for 2 h

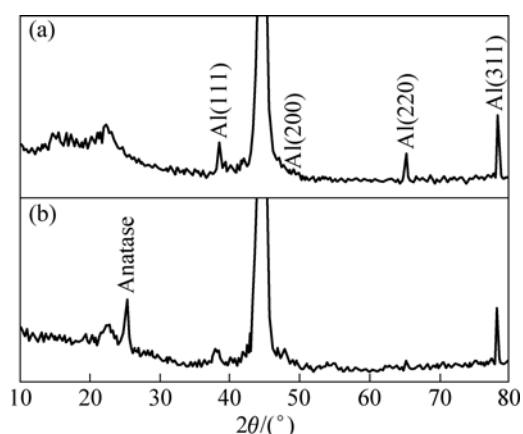
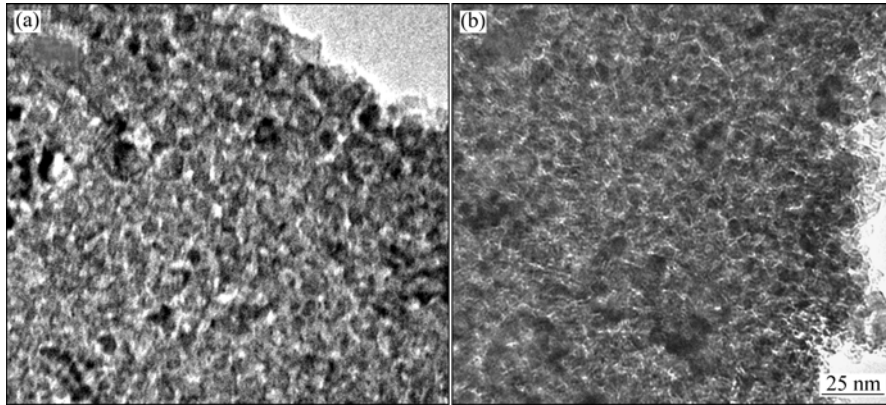


Fig.2 XRD patterns of specimen without TiO<sub>2</sub> (a), and after TiO<sub>2</sub> sol-gel dip-coating for 4 times (b)

### 3.2 Microstructure of TiO<sub>2</sub> coating and anodic oxide film

TEM images of TiO<sub>2</sub> coating are illustrated in Fig.3. The coating had a network structure of micro-pores and cracks which resulted from the evaporation of organic compounds during heating of the sol precursor film. By comparing Fig.3(a) with Fig.3(b), it was found that TiO<sub>2</sub> coating became denser obviously as coating times ( $n$ ) increased. Fig.4(a) shows TEM image of anodic oxide film formed on specimen with  $n=1$ , and a magnified image is illustrated in Fig.4(b). The network structure was not observed in Fig.4 since the TiO<sub>2</sub> coating was joined with Al anodic oxide film.

Fig.5 shows AES depth profiles of anodized specimens. It was indicated that an anodic oxide film formed between TiO<sub>2</sub> coating and Al substrate. The film showed a dual-layer structure: an inner layer of Al<sub>2</sub>O<sub>3</sub> and an outer layer of Ti-Al composite oxide. The thickness of anodic oxide film formed on specimens with TiO<sub>2</sub> was approximately 150 nm, while it was 180 nm for that without TiO<sub>2</sub>. Moreover, the thickness of TiO<sub>2</sub>



**Fig.3** TEM images of TiO<sub>2</sub> coating stripped from specimens before anodizing: (a)  $n=1$ ; (b)  $n=2$

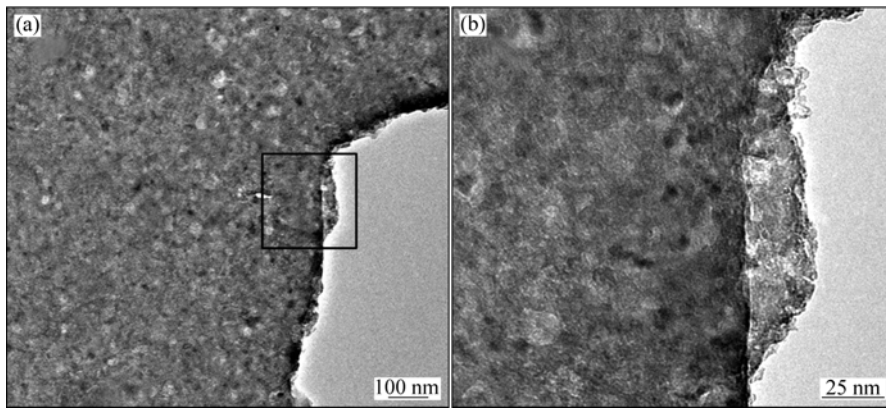


**Fig.4** TEM image of anodic oxide film stripped from anodized specimen with  $n=1$  (a), and magnified image of location in frame (b)

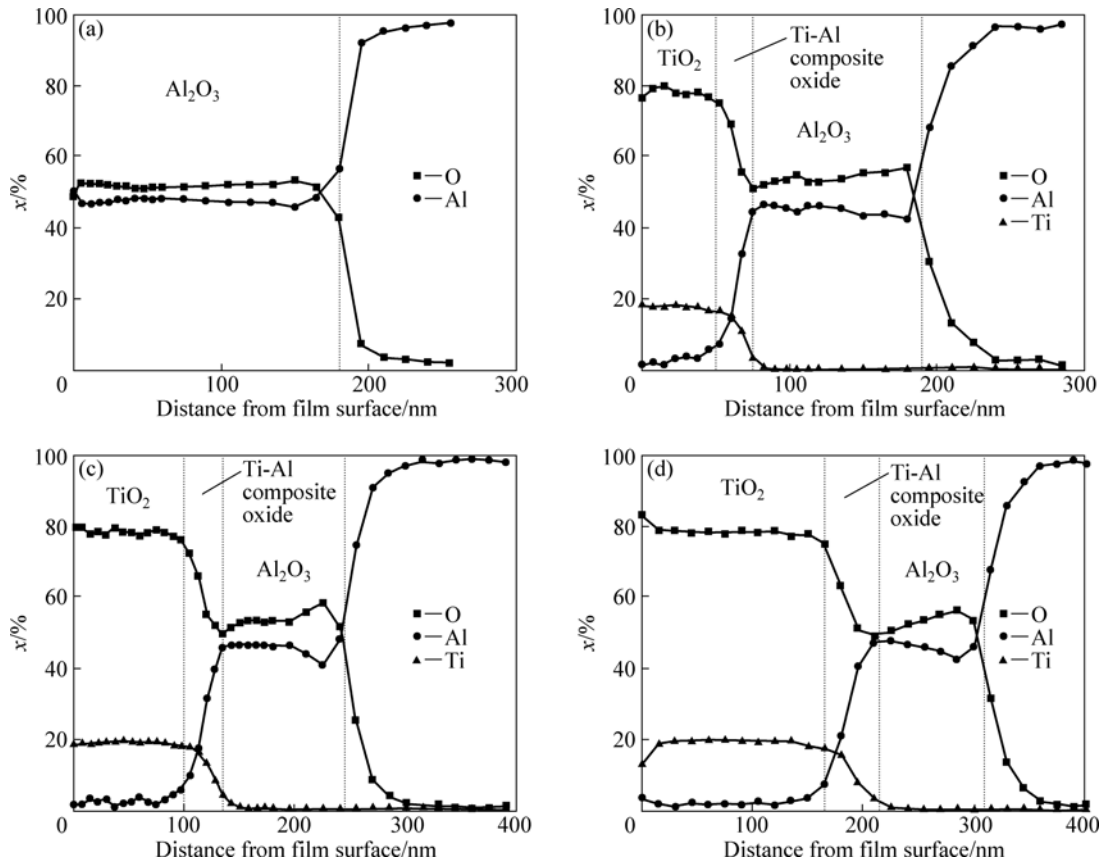


**Fig.5** Content depth profiles of O, Al and Ti of anodized specimens: (a) Without TiO<sub>2</sub>; (b)  $n=1$ ; (c)  $n=2$ ; (d)  $n=4$

coating increased from 50 nm to 160 nm as  $n$  increased from 1 to 4.

### 3.3 Effect of repeated sol-gel coating on anodic oxide film

Thickness variations of both layers in anodic oxide film are shown in Fig.6 and the specimen without  $\text{TiO}_2$  is represented as  $n=0$ . It was indicated that the thickness of inner layer,  $d_i$ , reduced from 120 nm to 100 nm and the thickness of outer layer,  $d_o$ , increased from 25 nm to 50 nm as  $n$  increased from 1 to 4.  $\text{TiO}_2$  sol-gel film caused the variation by inhibiting  $\text{Al}^{3+}$  and  $\text{O}^{2-}$  ions transport during the anodizing.

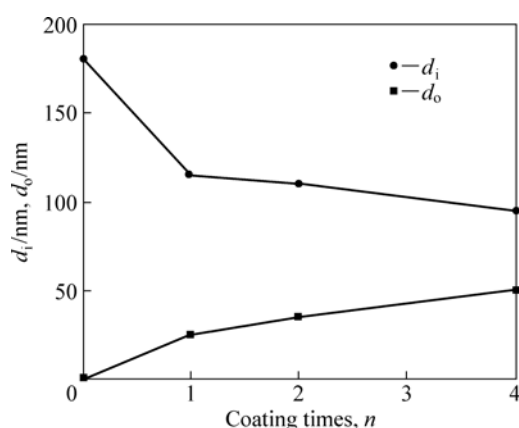


**Fig.6** Thickness variation of inner layer and outer layer with coating times

On the other hand, the total thickness of anodic oxide film showed not much difference even the  $\text{TiO}_2$  coating was 160 nm thick when  $n=4$ . Therefore, it was considered that  $\text{TiO}_2$  coating could not sustain voltage during the anodizing because of the strong local electric field. Similarly, TAKAHASHI et al[1] had concluded that Zr oxide sol-gel film could not sustain voltage during the anodizing of Al substrate.

### 3.4 Formation mechanism of Ti-Al composite oxide film

Fig.7 shows a model of the anodization of specimens with  $\text{TiO}_2$ . When the specimens were placed in the solution, water and electrolyte penetrated into the micro-pores network in the  $\text{TiO}_2$  coating and met the metal substrate. During the anodizing,  $\text{O}^{2-}$  anions dissociated from water at the bottom of the  $\text{TiO}_2$  layer transported inwards across the anodic oxide film to form  $\text{Al}_2\text{O}_3$  at the interface between the inner layer and Al substrate.  $\text{Al}^{3+}$  cations transported outwards and formed  $\text{Al}_2\text{O}_3$  in the micro-pores. Consequently, the composite oxide layer grown as the micro-pores in  $\text{TiO}_2$  coating were filled with  $\text{Al}_2\text{O}_3$ .

As shown in Fig.3 and Fig.5,  $\text{TiO}_2$  coating became thick and dense with more cycles of dip-coating. As a

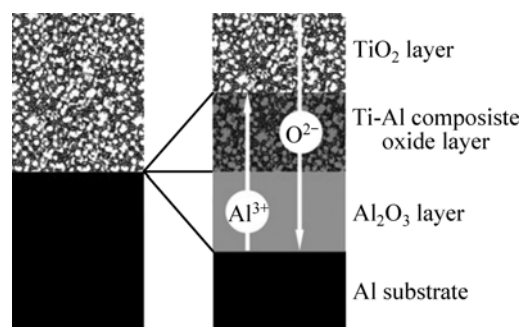


**Fig.7** Model of formation of dual layer structure of anodic oxide film on specimens with  $\text{TiO}_2$

result, the micro-pore network structure changed and it became more difficult for water and electrolyte to penetrate into a thicker  $\text{TiO}_2$  coating. Moreover, the denser  $\text{TiO}_2$  coating also inhibited  $\text{Al}^{3+}$  and  $\text{O}^{2-}$  ions transport during the anodizing. For these reasons, the growth speed of anodic oxide film was slowed down as  $n$  increased. The thickness variation of outer layer and inner layer with different  $n$  values could be explained as follows.  $\text{Al}^{3+}$  and  $\text{O}^{2-}$  ions transport resulted in the growth of the outer and inner layers.  $\text{Al}^{3+}$  cations formed Ti-Al composite oxide by filling the micro-pores in  $\text{TiO}_2$  coating with  $\text{Al}_2\text{O}_3$ . Thus, the formation of outer layer consumed electric charge and  $\text{Al}^{3+}$  only for repairing the cracks and voids in the  $\text{TiO}_2$  coating. When the inhibition on ions transport was enhanced as  $n$  increased, the growth speed ratio of the outer layer to the inner layer went up although growth of both layers was slowed down.

In conclusion, the formation and structure of anodic oxide film were mainly affected by the constitution of micro-pore network in  $\text{TiO}_2$  coatings which had an influence on ions transport. PARK and LEE[13] suggested that composite oxide film formed irrelevant to coating materials. This could be explained with above film formation mechanism.

### 3.5 Capacitance properties of anodic oxide film

Fig.8 shows Bode diagrams resulted from EIS measurements of anodized specimens. For all the specimens,  $\lg|Z|$  decreased linearly with a slope of  $-1$  in the high-frequency region and the curves became flat in the low-frequency region. The  $\lg|Z|$  vs  $\lg f$  curves of specimens with  $\text{TiO}_2$  turned into horizontal lines when frequency was less than 10 mHz and the horizontal lines located downwards as  $n$  increased. However, no horizontal line was observed on impedance curve of the specimen without  $\text{TiO}_2$ . The phase shift angle  $\theta$  vs  $\lg f$  curves of all specimens had a similar shape and shifted to high-frequency direction as  $n$  increased.

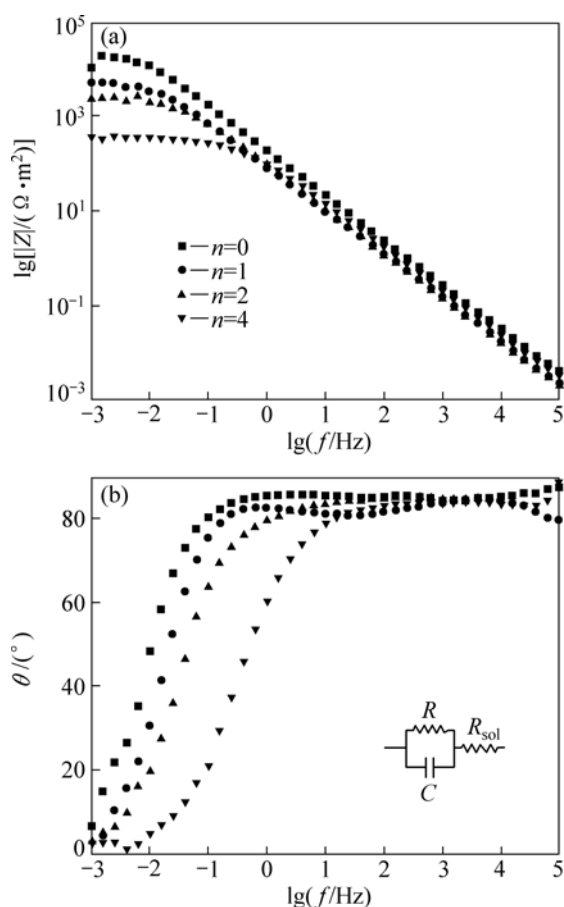


**Fig.8** Bode diagrams of anodized specimens: (a)  $\lg|Z|-\lg f$  curves; (b)  $\theta-\lg f$  curves

According to EIS data, equivalent electric circuit of all specimens could correspond to the one inserted in Fig.8. The symbols  $C$  and  $R$  represented the parallel capacitance and the parallel resistance of anodic oxide film, respectively. The symbol  $R_{sol}$  represented the solution resistance. Since  $R$  value was considerably larger than  $C$  and  $R_{sol}$ , the phase shift angle,  $\theta$ , was nearly  $90^\circ$  in wide frequency range and did not change until the frequency was low enough.

According to the equivalent electric circuit, calculated  $C$  value was commensurate to 62.4, 111.9, 112.6 and 75.6 nF/cm<sup>2</sup> for  $n=0, 1, 2, 4$ , respectively (shown in Fig.9). The results showed that the electric capacitance of anodic oxide film formed on specimens with TiO<sub>2</sub> was at most 80% higher than that without TiO<sub>2</sub>. The increase of  $C$  value was mainly due to higher dielectric constant of anodic oxide film which was incorporated with TiO<sub>2</sub>. On the other hand, sharp decrease in capacitance was noticed when dip-coating was repeated for four times. This is because TiO<sub>2</sub> film on the specimen with  $n=4$  was so thick and dense that its capacitance properties must not be omitted. According to Eq.(1), large  $C$  value was not obtained since  $d$  turned to be the total thickness of anodic oxide film and TiO<sub>2</sub>

coating. The specific capacitance,  $C_s$ , measured by LCR meter, is also presented in Fig.9 and it accorded with the EIS result.

The parallel resistance,  $R$ , determined leakage current through anodic oxide film under a certain voltage. The calculated  $R$  value was commensurate to  $1.6 \times 10^4$ ,  $4.4 \times 10^3$ ,  $2.3 \times 10^3$  and  $3.3 \times 10^2 \Omega \cdot m^2$  for  $n=0, 1, 2, 4$ , respectively (shown in Fig.10). It was indicated that the  $R$  value reduced with  $n$ , which showed coherence with the thickness variation of inner layer. Consequently, it was considered that the resistance of outer Ti-Al composite oxide layer was much less than that of the inner Al<sub>2</sub>O<sub>3</sub> layer. Since some micro-pores were not filled and remained, the outer layer had much more defects than the dense inner layer. These micro-pores permitted the electrolyte to penetrate into the dielectric film and resulted in the increment of leakage current.

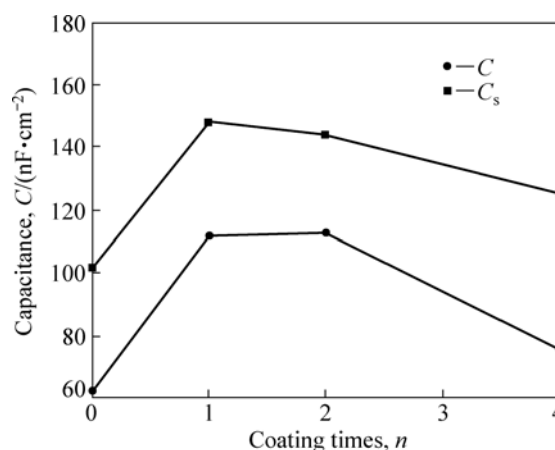


**Fig.9** Change in  $C$  and  $C_s$  of anodic oxide film with  $n$

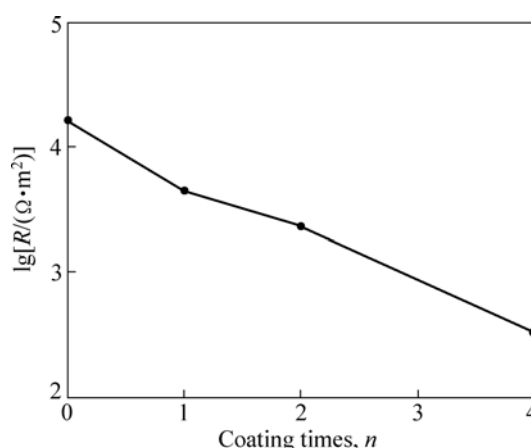


**Fig.10** Change in  $R$  of anodic oxide film with  $n$

### 4 Conclusions

1) Ti-Al composite oxide film was prepared on highly pure Al foil by using the method of sol-gel coating and subsequent anodizing. An anodic oxide film was obtained between TiO<sub>2</sub> coating and Al substrate. The

film showed a dual-layer structure consisting of an inner  $\text{Al}_2\text{O}_3$  layer and an outer Ti-Al composite oxide layer. The thickness of inner layer reduced and that of outer layer increased with more cycles of sol-gel dip-coating.

2) The inner layer grew at the interface between anodic oxide film and Al substrate, which resulted from the inward transport of  $\text{O}^{2-}$  anions. The outer layer grown as the micro-pores in  $\text{TiO}_2$  coating were filled with  $\text{Al}_2\text{O}_3$ , which resulted from the outward transport of  $\text{Al}^{3+}$  cations.  $\text{TiO}_2$  film caused the thickness variation of both layers by inhibiting  $\text{Al}^{3+}$  and  $\text{O}^{2-}$  transport during the anodizing.

3) The formation and structure of Al anodic oxide film were mainly affected by the constitution of micro-pore network in  $\text{TiO}_2$  coating.

4) The capacitance of anodic oxide film on specimens with  $\text{TiO}_2$  was at most 80% higher than that without  $\text{TiO}_2$ . On the other hand, the resistance of anodic oxide film reduced when multiplied dip-coating was applied.

## References

- [1] WATANABE K, SAKAIRI M, TAKAHASHI H, HIRAI S, YAMAGUCHI S. Formation of Al-Zr composite oxide films on aluminum by sol-gel coating and anodizing [J]. *Journal of Electroanalytical Chemistry*, 1999, 473: 250–255.
- [2] SHIKANAI M, SAKAIRI M, TAKAHASHI H, SEO M, TAKAHIRO K, NAGATA S, YAMAGUCHI S. Formation of Al/(Ti, Nb, Ta)-composite oxide films on aluminum by pore filling [J]. *Journal of the Electrochemical Society*, 1997, 144(8): 2756–2767.
- [3] WATANABE K, SAKAIRI M, TAKAHASHI H, HIRAI S, YAMAGUCHI S. Formation of composite oxide films on aluminum by sol-gel coating and anodizing—For the development of high performance aluminum electrolytic capacitors [J]. *Electrochemistry*, 2001, 69(6): 407–413.
- [4] WATANABE K, SAKAIRI M, TAKAHASHI H, TAKAHIRO K, NAGATA S, HIRAI S. Anodizing of aluminum coated with silicon oxide by a sil-gel method [J]. *Journal of the Electrochemical Society*, 2001, 148(11): B473–B481.
- [5] SUNADA M, TAKAHASHI H, KIKUCHI T, SAKAIRI M, HIRAI S. Dielectric properties of Al-Si composite oxide films formed on electropolished and DC-etched aluminum by electrophoretic sol-gel coating and anodizing [J]. *Journal of Solid State Electrochemistry*, 2007, 11: 1375–1384.
- [6] KOYAMA S, KIKUCHI T, SAKAIRI M, TAKAHASHI H, NAGATA S.  $\text{Nb}_2\text{O}_5$  deposition on aluminum from  $\text{NbCl}_5$ -used sol and anodizing of  $\text{Nb}_2\text{O}_5$ -coated Al [J]. *Electrochemistry*, 2007, 75(8): 573–575.
- [7] XU You-Long.  $\text{Al}_2\text{O}_3$ - $(\text{Ba}_{0.5}\text{Sr}_{0.5})\text{TiO}_3$  composite oxide films on etched aluminum foil by sol-gel coating and anodizing [J]. *Ceramics International*, 2004, 30: 1741–1743.
- [8] DU Xian-Feng, XU You-Long. Formation of  $\text{Al}_2\text{O}_3$ - $\text{Bi}_4\text{Ti}_3\text{O}_{12}$  nanocomposite oxide films on low-voltage etched aluminum foil by sol-gel processing [J]. *Surface and Coatings Technology*, 2008, 202: 1923–1927.
- [9] WANG Yin-Hua, YANG Jun, WANG Jian-Zhong.  $(\text{Ba}_{0.5}\text{Sr}_{0.5})\text{TiO}_3$  modification on etched aluminum foil for electrolytic capacitor [J]. *Ceramics International*, 2008, 34(5): 1285–1287.
- [10] KAMADA K, TOKUTOMI M, ENOMOTO N, HOJO J. Incorporation of oxide nanoparticles into barrier-type alumina film via anodic oxidation combined with electrophoretic deposition [J]. *Journal of Materials Chemistry*, 2005, 15: 3388–3394.
- [11] CHEN Jin-Ju, FENG Zhe-Sheng, YANG Bang-Chao.  $\text{Al}_2\text{O}_3$ - $\text{TiO}_2$  composite oxide films on etched aluminum foil by hydrolysis precipitation and anodizing [J]. *Journal of Materials Science*, 2006, 41: 569–571.
- [12] CHEN Jin-Ju, FENG Zhe-Sheng, JIANG Mei-Lian, YANG Bang-Chao. The effect of anodizing voltage on the electrical properties of Al-Ti composite oxide film on aluminum [J]. *Journal of Electroanalytical Chemistry*, 2006, 590: 26–31.
- [13] PARK S S, LEE B T. Anodizing properties of high dielectric oxide films coated on aluminum by sol-gel method [J]. *Journal of Electroceramics*, 2004, 13: 111–116.
- [14] BAILER J. *Comprehensive inorganic chemistry* [M]. New York: Pergamon Press, 1973: 373.
- [15] FALLET M, PERMPOON S, DESCHANVRES J L, LANGLET M. Influence of physico-structural properties on the photocatalytic activity of sol-gel derived  $\text{TiO}_2$  thin films [J]. *Journal of Materials Science*, 2006, 41: 2915–2927.

(Edited by YANG Bing)